Applied Science and Innovative Research
ISSN 2474-4972 (Print) ISSN 2474-4980 (Online)
Vol. 10, No. 2, 2026
www.scholink.org/ojs/index.php/asir

Original Paper

Adsorption of Methylene Blue and Congo Red by Silica Nanowires

Qing Li[1*]

[1] College of Materials and Chemistry & Chemical Engineering, Chengdu University of Technology, Chengdu, China

[*] E-mail: qing_li2026@126.com

Received: April 27, 2026 Accepted: May 19, 2026 Online Published: May 26, 2026

doi:10.22158/asir.v10n2p21 URL: http://dx.doi.org/10.22158/asir.v10n2p21

Abstract

Silica nanowires (SiO_2 NWs) were prepared via a PVP-Na_3Cit-TMOS system and used as adsorbents for the removal of methylene blue (MB) and Congo red (CR) from aqueous solutions. The adsorption of MB reached equilibrium within 20 min at 25 °C and pH 9.0, with a capacity of 155.0 mg/g, while CR achieved equilibrium within 45 min at 25 °C and pH 2.0, with a capacity of 60.8 mg/g. The adsorption processes followed the pseudo-second-order kinetic model and the Langmuir isotherm model, indicating monolayer physical adsorption. Thermodynamic parameters ($\Delta G < 0$, $\Delta H < 0$) confirmed spontaneous exothermic adsorption. pH played a critical role: alkaline conditions favored MB adsorption due to enhanced electrostatic attraction, whereas strongly acidic conditions promoted CR adsorption. The SiO_2 nanowires exhibited significantly higher affinity for the cationic dye MB, demonstrating promising potential for the treatment of cationic dye-contaminated wastewater.

Keywords

SiO_2 nanowires, Methylene blue, Congo red, Adsorption

1. Introduction

In recent years, water pollution has emerged as one of the most pressing global challenges, paralleling energy scarcity. Among various water pollutants, organic dyes have become particularly prominent due to their extensive use in the textile, plastics, leather, papermaking, and other industries. Dye-containing wastewater not only causes severe chromatic pollution, reduces light penetration, and disrupts aquatic ecosystems, but may also accumulate through the food chain, posing potential risks such as carcinogenicity and teratogenicity to organisms and human health.[1, 2]

Methylene Blue (MB), a representative cationic thiazine dye, and Congo Red (CR), a typical anionic azo

dye, are characterized by complex aromatic structures, high water solubility, strong biotoxicity, and resistance to natural degradation.[3-6]

Among various treatment technologies, adsorption has been widely applied for the removal of organic pollutants from wastewater owing to its operational simplicity, high efficiency, low cost, and minimal secondary pollution. The development of novel adsorbents with high adsorption capacity, rapid adsorption kinetics, and good regeneration performance remains a central research focus.[7]

In recent years, various nanomaterials-such as carbon nanotubes[8], graphene[9], metal oxides[10], and natural polymer-based nanocomposites[11]-have been extensively investigated as dye adsorbents. Compared with zero-dimensional nanoparticles, one-dimensional (1D) nanomaterials have attracted considerable attention in catalysis, sensing, energy, and environmental applications due to their unique anisotropic structures and excellent physicochemical properties. Notably, the entangled network formed by 1D nanostructures facilitates sedimentation and post-treatment, offering promising practical application potential.[12]

In this study, SiO_2 nanowires were employed as adsorbents to evaluate their removal performance toward cationic MB and anionic CR in aqueous solutions.

2. Experimental

2.1 Materials

Polyvinylpyrrolidone (PVP, Mw=10000, Shanghai Macklin Biochemical Technology Co., Ltd), sodium citrate (Shanghai Aladdin Chemistry Co., Ltd), tetra methoxy silane (TMOS, Beijing J&K Technology Co., Ltd), isopropanol (IPA) and ammonia (25%-28%, Chengdu Ke long Chemical Co., Ltd) were all used as received without any purification. Deionized water with a resistivity of 18.0 MΩ was used in all experiments. Methylene blue, (MB, Shanghai Macklin Biochemical Technology Co., Ltd), Congo red (CR, Shanghai Aladdin Chemistry Co., Ltd).

2.2 Preparation of SiO_2 Nanowires

SiO_2 nanowires with diameters of approximately 110 nm and lengths of 5μm were synthesized via an emulsion templating method. In a typical procedure, 0.01 g of PVP (M_W = 10,000) was dissolved in 5 mL of isopropanol within a sealed 10 mL centrifuge tube. The mixture was sonicated for 15 min until a clear homogeneous solution was obtained. Subsequently, 0.3 mL of deionized water, 0.2 mL of sodium citrate (0.25 M), and 0.2 mL of ammonia water (2 M) were sequentially added, with manual shaking after each addition. Finally, 0.05 mL of TMOS was introduced, and the mixture was thoroughly shaken. The reaction was conducted in a water bath at 50 °C for 2.5 h. After cooling to room temperature, the product was collected by centrifugation, washed three times with deionized water and twice with ethanol, dried at 80 °C, and finally calcined at 500 °C for 2 h, obtained SiO_2 nanowires with a yield of approximately 80%.

2.3 Experimental

A predetermined amount of SiO_2 nanowires was introduced into a 100 mL centrifuge tube containing a fixed volume of dye solution. The tube was securely sealed and subsequently transferred to a

constant-temperature water bath shaker, where the mixture was agitated continuously to ensure thorough contact between the adsorbent and the dye.

At specified time intervals, aliquots of the suspension were withdrawn using disposable syringes and immediately filtered through a 0.45 μm hydrophilic membrane to separate the solid phase. The filtrate was then analyzed using a UV-Vis spectrophotometer at the maximum absorption wavelength of the corresponding dye.

The equilibrium adsorption capacity *Qe* (mg/g) of the SiO_2 nanowires was calculated according to Equation (1), while the adsorption efficiency *R* (%) was determined using Equation (2).

$$Q_e = \frac{(C_0 - C_e) \times V}{m} \quad (1)$$

$$R = \frac{(C_0 - C_e)}{C_0} \times 100\% \quad (2)$$

where C_0 is the initial concentration of the dye (mg/L); *Ce* is the equilibrium concentration of the dye in solution (mg/L); *V* is the volume of the solution (mL); and *m* is the mass of SiO_2 nanowires used (mg).

3. Results and Discussion

3.1 The Influence of pH

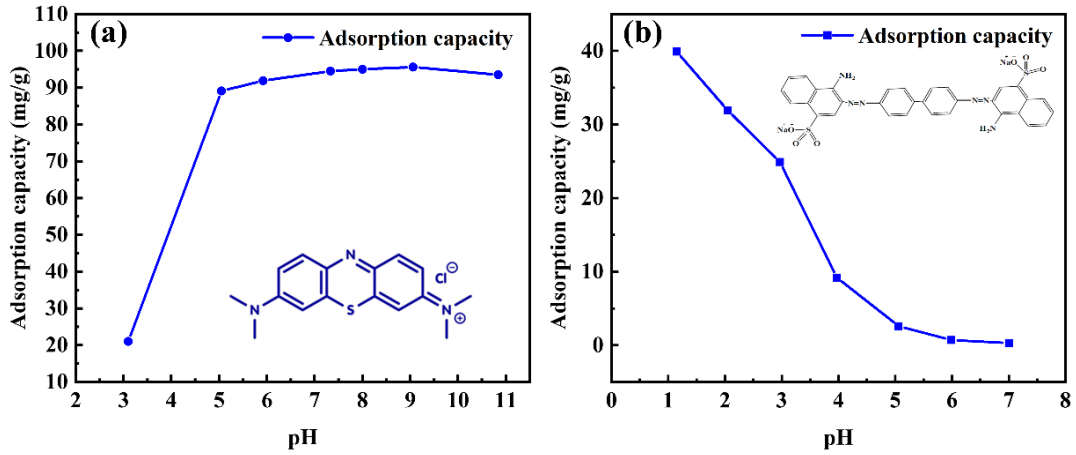

Figure 1. The Influence of pH on the Adsorption of MB and CR by SiO_2 Nanowires

(a: MB; b: CR)

(MB experimental conditions: 25 ℃, 20 minutes; Material addition amount: 50 mg; MB concentration: 100 mg/L; Solution volume: 50 mL. CR experimental conditions: 25 °C, 45 min; adsorbent dosage: 50 mg; CR concentration: 40 mg/L; solution volume: 50 mL. Data were the average values of three parallel adsorption experiments)

The effect of pH on MB and CR adsorption by SiO_2 nanowires was shown in Figure 1. For MB, adsorption capacity increased from 21.0 mg/g (pH 3.0) to 95.6 mg/g (pH 9.0), then plateaued. Under neutral to alkaline conditions, deprotonated silanol groups (≡Si-O^-) electrostatically attract cationic MB^+,

while hydrogen bonding between MB and Si-OH further enhances adsorption. Under acidic conditions, electrostatic attraction weakens, and adsorption relies on weaker interactions (e.g., hydrogen bonding and van der Waals forces).

For CR, adsorption capacity decreased sharply with increasing pH: 38.1 mg/g at pH 1.0, 0.7 mg/g at pH 6.0, and 0.3 mg/g at pH 7.0. The point of zero charge (PZC) of SiO_2 nanowires is approximately 2-3[13] and the pKa values of CR are 3.70 and 5.40. At pH < PZC, the nanowire surface is positively charged ($\equiv Si\text{-}OH_2^+$), leading to strong electrostatic attraction with anionic CR. At pH ≥ 5, the negatively charged surface ($\equiv Si\text{-}O^-$) repels CR, resulting in a sharp decline in adsorption capacity.

3.2 The Influence of Adsorption Temperature and Time

Figure 2a showed the adsorption kinetics of MB onto SiO_2 nanowires at different temperatures. At 25 °C, equilibrium was reached within 20 min, with an adsorption capacity of 90.8 mg/g and a removal efficiency of 95.0 %. Increased the temperature to 35 °C and 45 °C shortened the equilibrium time to 10 min and 5 min, respectively, but decreased the adsorption capacity to 85.7 mg/g and 84.5 mg/g, and removal efficiency to 85.0 % and 84.0 %. The decreasing adsorption capacity with increasing temperature indicates an exothermic adsorption process.

Figure 2b presents the adsorption kinetics of CR onto SiO_2 nanowires at different temperatures. At 25 °C, equilibrium was reached at 45 min, with an adsorption capacity of 24.8 mg/g and a removal efficiency of 66.0 %. At 35 °C and 45 °C, the equilibrium time decreased to 35 min and 25 min, while the adsorption capacity decreased to 23.5 mg/g and 21.4 mg/g, with removal efficiencies of 60.0 % and 55.0 %, respectively. Similar to MB, the adsorption of CR is also an exothermic process.

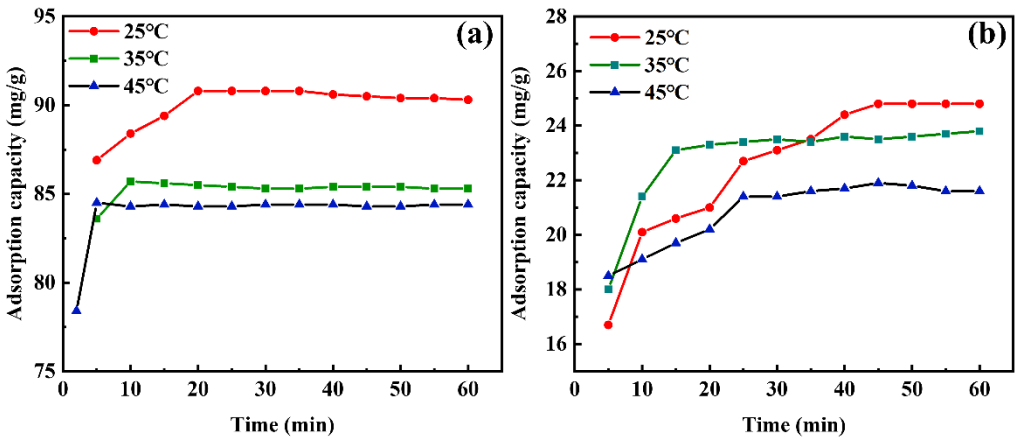

Figure 2. The Adsorption Kinetics Curve of MB and CR by SiO_2 Nanowires

(a: MB; b: CR)

(MB experimental conditions: Initial pH: 7.33; Material addition amount: 50 mg; MB concentration: 100 mg/L; Solution volume: 50 mL. CR experimental conditions: pH: 2.0; adsorbent dosage: 50 mg; CR concentration: 40 mg/L; solution volume: 50 mL. Data were the average values of three parallel adsorption experiments)

3.3 The Saturated Adsorption Amounts at Different Temperatures

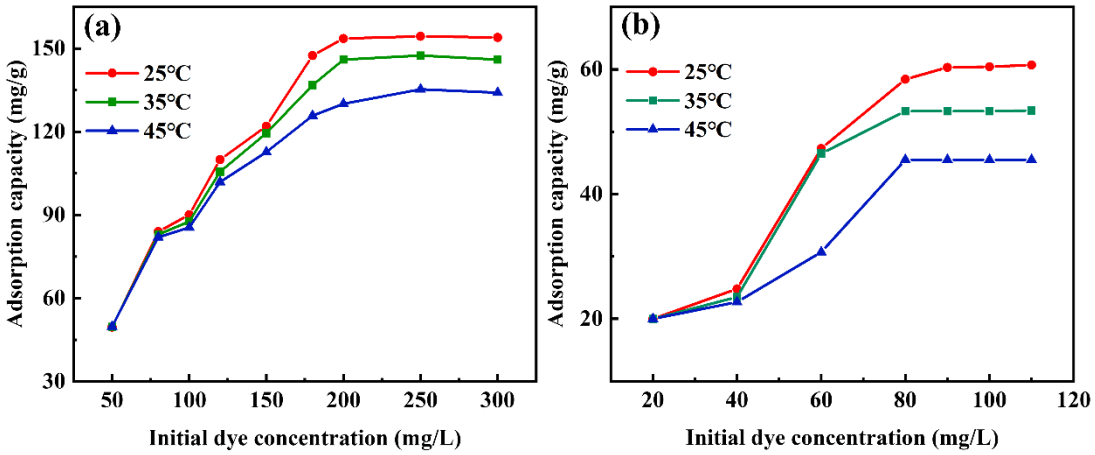

Figure 3. The Adsorption Isotherm of MB and CR by the SiO_2 Nanowires

(a: MB; b: CR)

(MB experimental conditions: Adsorption time: 20 minutes; Initial pH: 7.33; Material dosage: 50 mg; Solution volume: 50 mL. CR experimental conditions: Adsorption time: 45 min; pH: 2.0; adsorbent dosage: 50 mg; solution volume: 50 mL. Data represents the average value of three parallel adsorption experiments)

Figure 3a showed the adsorption isotherms of MB onto SiO_2 nanowires at different temperatures. In the low concentration range (50-200 mg/L), the adsorption capacity increased sharply with increasing MB concentration due to the enhanced concentration gradient and abundant active sites. Beyond 200 mg/L, the adsorption gradually approached saturation. The maximum adsorption capacities decreased with increasing temperature: 155.0 mg/g at 25 °C, 148.0 mg/g at 35 °C, and 135.3 mg/g at 45 °C, indicating an exothermic adsorption process with 25 °C being the optimal temperature.

Figure 3b presents the adsorption isotherms of CR onto SiO_2 nanowires at different temperatures. In the low concentration range, the adsorption capacity increased rapidly with initial CR concentration, then leveled off beyond 80 mg/L as saturation was reached. The saturated adsorption capacities decreased significantly with increasing temperature: 60.8 mg/g at 25 °C, 53.4 mg/g at 35 °C, and 45.5 mg/g at 45 °C, also indicating an exothermic process.

3.4 Adsorption Kinetic Curve

According to the data, under three different temperature conditions (as shown in Figure 2), the adsorption capabilities of MB and CR on the silicon nanowires changed over time. To gain deeper insight into the adsorption mechanism of MB and CR onto the SiO_2 nanowires, three widely used kinetic models-the pseudo-first-order, pseudo-second-order, and intraparticle diffusion models-were employed to fit the experimental data. The corresponding fitting results are summarized in Tables 1 to 2.

The pseudo-first-order model is expressed as:

$$Q_t = Q_e(1 - e^{-k_1 t}) \quad (3)$$

Where *Qe* and *Qt* (mg/g) represent the adsorption capacity of the adsorbent material toward MB and CR at adsorption equilibrium and at a given time *t* during the adsorption process, respectively; *t* is the adsorption time (min); and k_1 (min^{-1}) is the rate constant of the pseudo-first-order kinetic model. k_1 can be obtained from the slope of the fitted line when plotting *Qe* versus *t* (as shown in Figure 4a, 5a).

The expression of the pseudo-second-order kinetic model is as follows:

$$\frac{t}{Q_t} = \frac{1}{k_2 Q_e^2} + \frac{t}{Q_e} \tag{4}$$

Where k_2 ($g \cdot mg^{-1} \cdot min^{-1}$) represents the adsorption rate constant of the pseudo-second-order kinetic model. Both k_2 and *Qe* can be calculated from the intercept and slope of the plot of *t/Qt* versus *t* (Figure 4b, 5b).

The rate-controlling step in the adsorption process was further identified by fitting the intraparticle diffusion model. The expression of the intraparticle diffusion model is as follows:

$$Qt = k_i t^{1/2} + C \tag{5}$$

Where k_i ($mg \cdot g^{-1} \cdot min^{-1/2}$) represents the intraparticle diffusion rate constant, and *C* (mg/g) represents the thickness of the boundary layer. Both k_i and *C* can be calculated from the intercept and slope of the plot of *Qt* versus $t^{1/2}$ (Figure 4c, 5c).

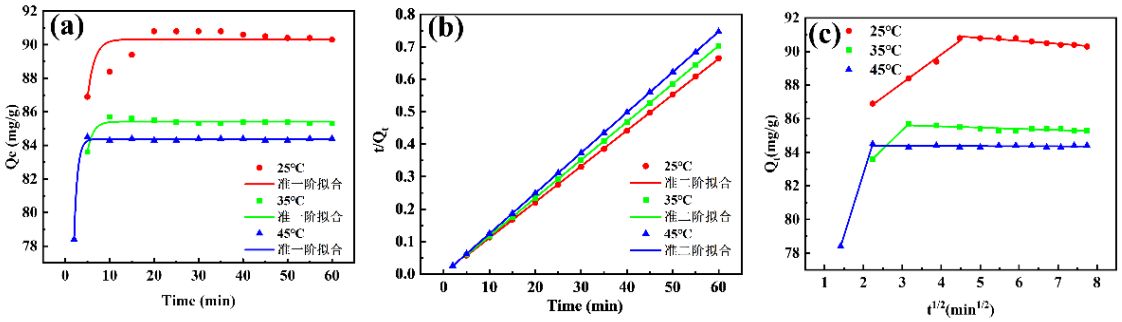

Figure 4. The Kinetic Model Fitting of SiO_2 Nanowires Adsorption of MB

(a: First-order approximation; b: Second-order approximation; c: Internal diffusion)

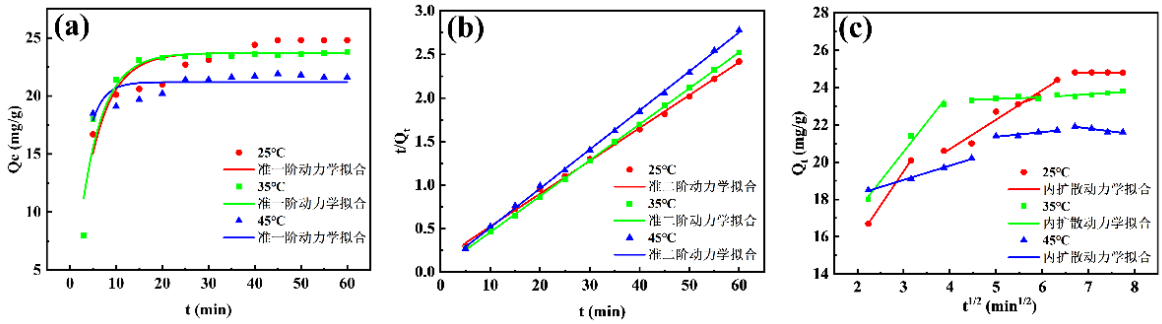

Figure 5. The Kinetic Model Fitting of SiO_2 Nanowires Adsorption of CR

(a: First-order approximation; b: Second-order approximation; c: Internal diffusion)

Table 1. Fitted Parameters of the Quasi-second-order Kinetic Model of MB

Temperature	R^2	Q_e（mg/g）	K_2
25℃	0.9999	90.7	0.11
35℃	0.9999	85.3	0.42
45℃	0.9999	80.4	0.73

Table 2. Fitted Parameters of the Quasi-second-order Kinetic Model of CR

Temperature	R^2	Qe（mg/g）	K_2
25℃	0.998	26.5	0.01
35℃	0.999	24.2	0.03
45℃	0.999	22.2	0.04

The adsorption kinetics of MB onto SiO_2 nanowires followed the pseudo-second-order model ($R^2 > 0.999$), indicating that the adsorption rate is controlled by the availability of surface active sites, and the adsorption capacity is determined by the total number of these sites. The intraparticle diffusion model (Figure 4c) revealed two distinct stages: Stage 1-combined boundary layer and intraparticle diffusion control; Stage 2-adsorption equilibrium. None of the fitted lines passed through the origin, suggesting that intraparticle diffusion is not the sole rate-controlling step.

The adsorption of CR also followed the pseudo-second-order model ($R^2 > 0.998$), indicating rate control by surface Si-OH groups. The intraparticle diffusion model (Figure 5c) revealed three distinct stages: Stage 1-boundary layer diffusion; Stage 2-intraparticle diffusion; Stage 3-adsorption equilibrium. None of the fitted lines passed through the origin, indicating that intraparticle diffusion is not the sole rate-controlling step. The adsorption rate of CR was significantly slower than that of MB. The fitting parameters of the quasi-second-order kinetic model for MB and CR were shown in Tables 1-2.

3.5 Adsorption Isothermal Model

Based on the data showing the adsorption capacity of MB and CR onto SiO_2 nanowires as a function of MB and CR concentration under three different temperature conditions (as shown in Figure 5), Langmuir and Freundlich isotherm model fittings were performed (Equation 6 and 7). The corresponding fitting equations and parameters are presented in Figure 6-7 and Tables 3-4.

The expression of the Langmuir model is as follows:

$$\frac{C_e}{Q_e} = \frac{1}{Q_m K_L} + \frac{C_e}{Q_m} \quad (6)$$

The expression of the Freundlich model is as follows:

$$lnQ_e = lnK_F + \frac{1}{n} lnC_e \quad (7)$$

In the formula:

Q_e-The adsorption amount of dye by the material at the adsorption equilibrium state (mg/g);

C_e-The concentration of dye in the solution at the adsorption equilibrium stage (mg/L);

Q_m- The maximum adsorption capacity of the material for dye (mg/g);

K_L- Langmuir isothermal equation adsorption equilibrium constant (L/mg);

K_F and $1/n$- Freundlich isothermal equation adsorption equilibrium constant (L/g) and exponent.

As shown in Figure 6, the correlation coefficients of the Langmuir model at all three temperatures are significantly higher than those of the Freundlich model, indicating that the adsorption of MB onto the SiO_2 nanowires follows a monolayer adsorption mode, with adsorption occurring primarily on the active sites on the material surface. The maximum adsorption capacities calculated by the Langmuir model at 25 °C, 35 °C, and 45 °C (157.5, 150.6, and 137.9 mg/g, respectively) are in good agreement with the experimental values (155.0, 148.0, and 135.3 mg/g). The specific parameters can be found in Table 3.

As shown in Figure 7, the correlation coefficients of the Langmuir isotherm model for CR adsorption onto the SiO_2 nanowires at the three temperatures are significantly higher than those of the Freundlich isotherm model. This indicates that the adsorption of CR onto the material follows a monolayer adsorption mode, with the majority of target molecules being adsorbed onto the active sites on the material surface. The maximum adsorption capacities calculated using the Langmuir isotherm model at 25 °C, 35 °C, and 45 °C were 62.4, 53.9, and 45.9 mg/g, respectively, which are in good agreement with the experimental values of 60.8, 53.4, and 45.5 mg/g. The specific parameters can be found in Table 4.

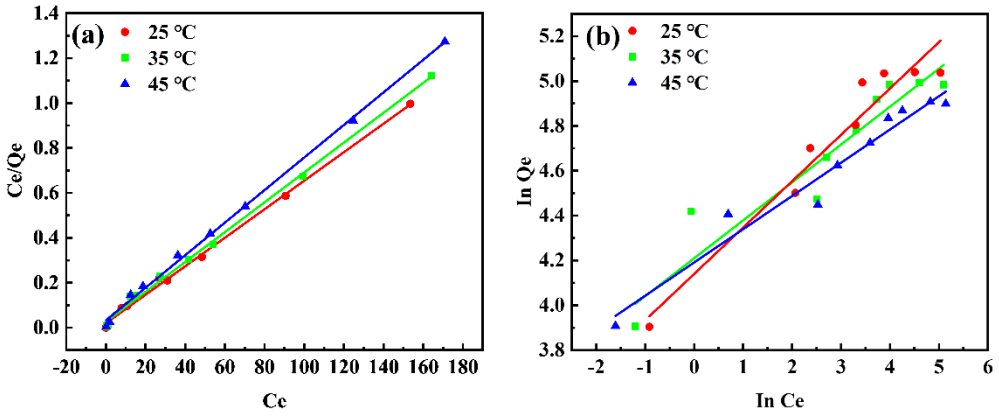

Figure 6. Linear Fitting of the Isothermal Adsorption Model for SiO_2 Nanowires to Adsorb MB

(a: Langmuir; b: Freundlich)

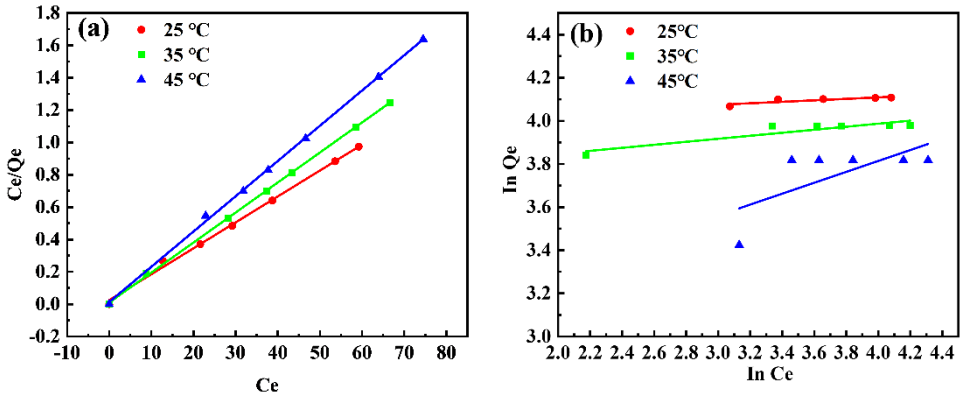

Figure 7. Linear Fitting of the Isothermal Adsorption Model for SiO_2 Nanowires to Adsorb CR

(a: Langmuir; b: Freundlich)

Table 3. Langmuir Isotherm Model Fitting Equation and Parameters of MB

Temperature	Fitted equation	R^2	$Q_{m\ cal}$	K_L
25°C	Y=0.00635x+0.01972	0.997	157.5	0.32
35°C	Y=0.00664x+0.02682	0.997	150.6	0.25
45°C	Y=0.00725x+0.03267	0.998	137.9	0.22

Table 4. Langmuir Isotherm Model Fitting Equation and Parameters of CR

Temperature	Fitted equation	R^2	$Q_{m\ cal}$	K_L
25°C	Y=0.01603x+0.02477	0.997	62.4	1.60
35°C	Y=0.01855x+0.02000	0.999	53.9	0.93
45°C	Y=0.02179x+0.02700	0.998	45.9	0.81

3.6 Adsorption Thermodynamics

Adsorption processes are usually accompanied by changes in heat. The functional relationships among the thermodynamic parameters-Gibbs free energy change ΔG (kJ/mol), enthalpy change ΔH (kJ/mol), and entropy change ΔS (J/(mol·K))-and the adsorption equilibrium constant as well as temperature are expressed as follows:

$$\Delta G = -RTlnK \quad (8)$$

$$lnK = -\frac{\Delta H}{RT} + \frac{\Delta S}{R} \quad (9)$$

In the formula:

K- adsorption equilibrium constant;

T- temperature (*K*);

R- perfect gas constant (8.314 *J/(mol·K)*).

The equilibrium constant *K* was calculated by linearly fitting *ln (Qe/Ce)* versus *Qe* (Figure 8a, 9a). Then, *ΔG* was calculated according to Equation 8, and a linear fit of *ln K* versus *1/T* was performed according to Equation 9 (Figure 8b, 9b), from which *ΔH* and *ΔS* were calculated using the obtained regression equation. The thermodynamic parameters for the adsorption of MB and CR onto the SiO_2 nanowires are presented in Tables 5 and 6.

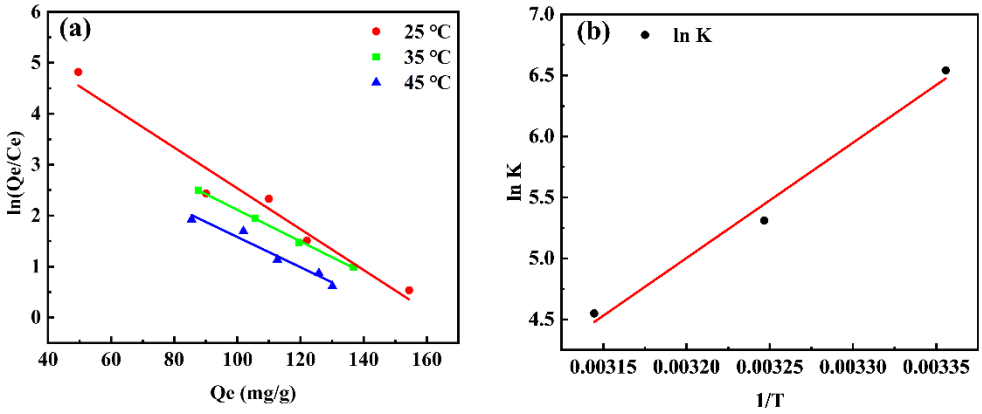

Figure 8. Thermodynamic Parameters of SiO_2 Nanowires for Adsorbing MB

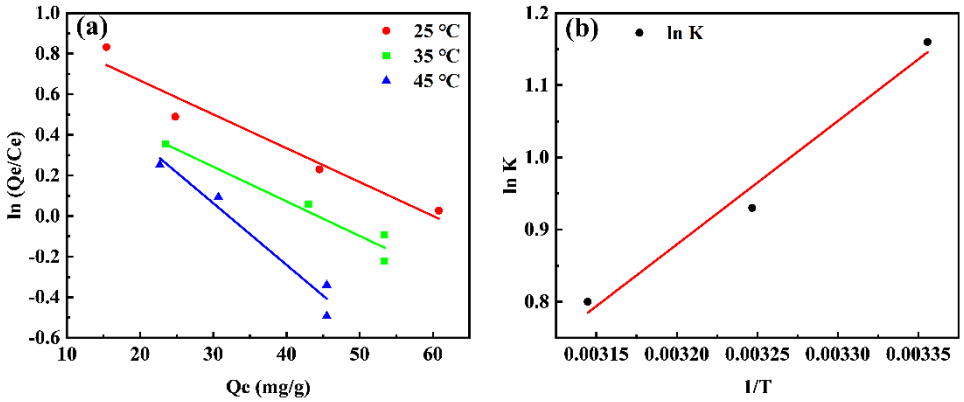

Figure 9. Thermodynamic Parameters of SiO_2 Nanowires for Adsorbing CR

(a: Calculate the equilibrium constant *K* by performing a linear regression on *ln Qe/Ce* data; b: Calculate thermodynamic parameters by performing a linear fitting of *ln K* against *1/T*)

As shown in Figure 8 and Table 5, the negative *ΔG* values (ranging from -20 to 0 kJ/mol) indicate that MB adsorption was a spontaneous process. Combined with the pH-dependent adsorption results (Figure 3a), this suggests physical adsorption. The *ΔH* value is -78.54 kJ/mol, and *ΔS* was negative, confirming an exothermic process with increased order at the solid-liquid interface. Elevated temperatures are unfavorable for adsorption.

As shown in Figure 9 and Table 6, the adsorption of CR exhibits $\Delta G < 0$ and $\Delta H < 0$ at 298, 308, and 318 *K*, indicating a spontaneous and exothermic process. The *ΔG* values range from -20 to 0 *kJ/mol*, and

together with the pH-dependent results (Figure 1b), this confirms physical adsorption. The negative *ΔS* indicates a decrease in system disorder during adsorption.

Table 5. Thermodynamic Parameters of the Adsorption Process of MB

T (*K*)	*ln K*	*ΔG (KJ/mol)*	*ΔH (KJ/mol)*	*ΔS (J/(mol·K))*
298	6.54	-16.20		
308	5.31	-13.60	-78.54	-209.7
318	4.55	-12.03		

Table 6. Thermodynamic Parameters of Material Adsorption of CR

T (K)	*ln K*	*ΔG (KJ/mol)*	*ΔH (KJ/mol)*	*ΔS (J/(mol·K))*
298	1.16	-2.87		
308	0.93	-2.38	-14.22	-38.18
318	0.80	-2.12		

4. Conclusion

In summary, SiO_2 nanowires synthesized by the PVP-Na_3Cit-TMOS method effectively adsorb both cationic MB and anionic CR. MB adsorption is optimal under neutral to alkaline conditions (pH 9.0) via electrostatic attraction, while CR adsorption is optimal under strongly acidic conditions (pH 1.0). Both adsorption processes follow pseudo-second-order kinetics and Langmuir isotherm, indicating monolayer adsorption on active sites. Thermodynamic parameters ($\Delta G < 0$, $\Delta H < 0$, $\Delta S < 0$) confirm spontaneous, exothermic physical adsorption with higher capacity at lower temperatures. The maximum adsorption capacities at 25 °C are 155.0 mg/g for MB and 60.8 mg/g for CR, demonstrating that SiO_2 nanowires are promising adsorbents for dye removal from wastewater.

References

[1] Al-Tohamy, R., Ali, S. S., Li, F., et al., (2022). A critical review on the treatment of dye-containing wastewater: Ecotoxicological and health concerns of textile dyes and possible remediation approaches for environmental safety. *Ecotoxicology and Environmental Safety*, *231*, 113160. http://dx.doi.org/10.1016/j.ecoenv.2021.113160

[2] Khan, S., Noor, T., Iqbal, N., et al., (2024). Photocatalytic dye degradation from textile wastewater: a review. *ACS Omega*, *9*, 21751-21767. http://dx.doi.org/10.1021/acsomega.4c00887

[3] Yaseen, D. A., & Scholz, M. (2018). Textile dye wastewater characteristics and constituents of synthetic effluents: a critical review. *International Journal of Environmental Science and Technology*, *16*, 1193-1226. http://dx.doi.org/10.1007/s13762-018-2130-z

[4] Chen, K., Feng, Q., Ma, D., et al. (2021). Hydroxyl modification of silica aerogel: An effective

adsorbent for cationic and anionic dyes. *Colloids and Surfaces A: Physicochemical and Engineering Aspects*, 616. http://dx.doi.org/10.1016/j.colsurfa.2021.126331

[5] Parida, S., Mandal, A. K., Behera, A. K., et al. (2025). A comprehensive review on phycoremediation of azo dye to combat industrial wastewater pollution. *Journal of Water Process Engineering*, 70. http://dx.doi.org/10.1016/j.jwpe.2025.107088

[6] Ali, I. H. (2021). Removal of Congo Red Dye From Aqueous Solution Using Eco-Friendly Adsorbent of Nanosilica. *Baghdad Science Journal*, 18 http://dx.doi.org/10.21123/bsj.2021.18.2.0366

[7] Hu, Q., & Hao, L. (2025). Adsorption Technologies in Wastewater Treatment Processes. *Water*, 17. http://dx.doi.org/10.3390/w17152335

[8] Ceroni, L., Benazzato, S., Pressi, S., et al. (2024). Enhanced adsorption of methylene blue dye on functionalized multi-walled carbon nanotubes. *Nanomaterials (Basel)*, *14*, 522. http://dx.doi.org/10.3390/nano14060522

[9] Vassileva, P., Tumbalev, V., Kichukova, D., et al. (2023). Study on the dye removal from aqueous solutions by graphene-based adsorbents. *Materials (Basel)*, *16*, 5754. http://dx.doi.org/10.3390/ma16175754

[10] Senthil Rathi, B., Ewe, L. S., S, S., et al. (2024). Recent trends and advancement in metal oxide nanoparticles for the degradation of dyes: synthesis, mechanism, types and its application. *Nanotoxicology*, *18*, 272-298. http://dx.doi.org/10.1080/17435390.2024.2349304

[11] Matter, E.A., Hassan, A.F., Elfaramawy, N.M., et al., (2024). Fabrication of nanocellulose/chitosan nanocomposite based on loofah sponge for efficient removal of methylene blue: thermodynamic and kinetic investigations. *Journal of Inorganic and Organometallic Polymers and Materials*, *34*, 5620-5635. http://dx.doi.org/10.1007/s10904-024-03150-z

[12] Zhang, L., He, W., Yuan, H., et al. (2024). Superlong metal-organic framework nanowire fabricated via steam-assisted conversion. *Chemistry*, *30*, e202401903. http://dx.doi.org/10.1002/chem.202401903

[13] Zhivkov, A. M., Popov, T. T., & Hristova, S. H. (2023). Composite hydrogels with included solid-state nanoparticles bearing anticancer chemotherapeutics. *Gels*, *9*, 421. http://dx.doi.org/10.3390/gels9050421